On the multi-fluid approach to multiphase flow modeling in hydraulic fracturing applications

Andrei A. Osiptsov

a.osiptsov@skoltech.ru

Abstract

In this review paper, we present a family of closely related models for multiphase flows at all stages of the technology of hydraulic fracturing, which is used for stimulation of production from oil and gas wells. The models are derived from conservation laws using asymptotic methods in the multi-fluid approach. Five separate problem formulations are distinguished: (i) suspension flow down the well, (ii) suspension flow and sedimentation in a hydraulic fracture, (iii) inertial migration of particles in the horizontal section of a vertical hydraulic fracture, (iv) filtration of fluid with fine particles through a random close pack of proppant in a closed hydraulic fracture, and, finally, (v) a gas-liquid flow in a well during cleanup and startup after the end of hydraulic fracturing. Advantages and drawbacks of the multi-fluid approach are discussed, in comparison to simplified semi-empirical effective-fluid and drift-flux models.

1 Introduction

The technology of hydraulic fracturing of a hydrocarbon bearing underground formation is based on injecting a fluid laden with rigid particles under a high pressure (up to several hundred bar) into the well to create fractures in the porous medium, which are filled with particles. After the end of pumping, fractures closed on packed granular material provide high-conductivity channels to transport hydrocarbons from reservoir to the well and all the way up to the surface. The well may be vertical (when a single bi-wing fracture is formed) or near-horizontal with several perforation clusters providing reservoir contact (the so-called multi-stage fracturing in low-permeability formations). The latter case gives rise to several transversal fractures.

With respect to different stages of the hydraulic fracturing technology, we consider four classes of multiphase flows that can be modelled within the multi-continua (or multi-fluid) approach [1]. In a more detail, we distinguish the following classes: (i) the flow of suspension of fluid with particles in a circular pipe at high Reynolds numbers during pumping, (ii) the flow of suspension in a narrow vertical hydraulic

fracture at moderate Re during pumping [2, 3], (iii) suspension filtration through a packed of proppant particles in a closed fracture during cleanup [4], and (iv) multiphase gas-liquid flow with admixture of rigid particles in a circular pipe during well start-up, cleanup and testing in a wide range of the Reynolds numbers [5]. We discuss the advantages and limitations of the multi-fluid approach based on the simulation examples from each of the four classes of multiphase flows, in comparison with simplified semi-empirical approaches, e.g. the drift-flux model for well flows, the effective-fluid model for suspension transport in fractures, and the deep-bed filtration model. The talk ends up with recommendations for future research on the topic. A detailed review of the state of the art in numerical modeling of hydraulic fracturing can be found in [7], and the most recent review with a specific focus on fluid mechanics of hydraulic fracturing is [6].

2 Two-fluid model for suspension transport in a fracture

In this section, we present in a lumped form the two-fluid model for suspension flow and sedimentation in a hydraulic fracture. This model was derived in the multi-continua approach [1] using asymptotic methods in the lubrication approximation. The key assumption is that the width-to-length ratio of the fracture is a small parameter: $\varepsilon = w/L \ll 1$. The cross-flow particle concentration profile is assumed uniform. In the width-averaged variables, the equations are as follows [2]:

$$\frac{\partial wC}{\partial t} + \nabla \left(wC\mathbf{V}_p \right) = 0 \quad (1)$$

$$\frac{\partial w}{\partial t} = \nabla \left[\frac{w^3}{12\mu(C)} \left(\nabla P + \mathrm{Bu} \left[1 + C(\eta - 1) \right] \mathbf{e}_2 \right) - wC\mathbf{V}_s \right] - 2v_l \quad (2)$$

$$\mathbf{V}_f = -\frac{w^2}{12\mu(C)} \left(\nabla P + \mathrm{Bu} \left[1 + C(\eta - 1) \right] \mathbf{e}_2 \right), \ \mathbf{V}_p = \mathbf{V}_f + \mathbf{V}_s \quad (3)$$

$$\mathbf{V}_s = -\frac{\mathrm{St}}{\mathrm{Fr}^2} \left(\frac{\eta - 1}{\eta} \right) f(C)\mathbf{e}_2, \ f(C) = \left(1 - \frac{C}{C_{max}} \right)^5, \ \mu(C) = \left(1 - \frac{C}{C_{max}} \right)^{-1.89}.$$

$$\mathrm{Bu} = \frac{\rho_f^0 g L^2}{\mu_0 U}, \quad \rho_p^0 / \rho_f^0.$$

Here, Cartesian coordinate system Oxy is introduced in the cell plane, so that y-axis (with the basis vector $\mathbf{e}_2$) is vertical and origin O is located in the bottom left corner of the computational domain; C is the particle volume fraction; $w(x, y, t)$ is the width of the fracture (in hydraulic fracturing simulators, the width is available from solving the geomechanics problem of fracture growth [7]); $\mathbf{V}_f$, $\mathbf{V}_p$, $\mathbf{V}_s$ are the width-averaged velocities of the fluid and the particles, and the settling velocity of particles relative to the fluid; v_l is the velocity of fluid leak-off through the porous walls; differential operator '∇' acts in the (x, y) plane as we applied the averaging procedure along the cell width. The flow scales are as follows: L is the cell length, U is the scale of the injection velocity, d is the cell width scale, ρ_0^f is the fracturing fluid density, μ_0 and τ_0 are the fracturing fluid plastic viscosity and yield stress, respectively; g is the gravity acceleration; Bu is the Buoyancy number.

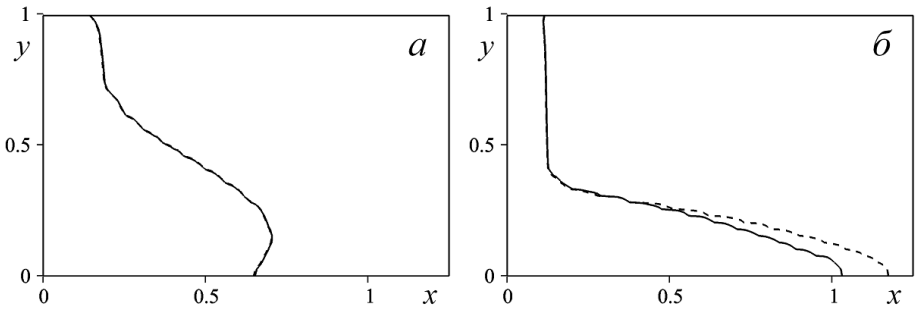

Figure 1: Particle concentration fronts in the fracture of elliptic cross-section at $t = 0.5$ for $Bu = 326$ (a) and $Bu = 3260$ (b). Result are obtained by the effective-fluid model (dashed line) and the two-fluid model (solid line).

Boundary and initial conditions for the hyperbolic equation for concentration (1) are given by:

$$t = 0 : C = 0, (x, y) \in [0, L/H] \times [0, 1]; \quad x = 0 : \; C = C_0, \, y \in [y_1, \, y_2]$$

Boundary conditions for the pressure equation (2) are as follows:

$$x = 0 : \; \frac{\partial p}{\partial x} = -\frac{12\mu\,(C)}{w^2}, \; y \in [y_1, \, y_2]; \; \frac{\partial p}{\partial x} = 0, y \in [0, \, y_1], [y_2, \, 1]$$

$$x = L/H : \; \frac{\partial p}{\partial y} = -\mathrm{Bu}; \quad y = 0, \; 1 : \; \frac{\partial p}{\partial y} = -\mathrm{Bu}(1 + C|_{y=0,\,1}(\eta - 1))$$

The particle settling velocity is given by an empirical formula, which is the generalization of the well-known Richardson-Zaki expression, taking into account the fact that particles slow down and stop completely when reaching the packed bed on the bottom. The existing effective-fluid models of suspension flows [8] contain an assumption that the *volume-averaged* suspension velocity is governed by the Poiseuille law, while in the present two-fluid model it is shown based on the derivation from the conservation laws that the Poiseuille law governs the *mass-averaged* velocity of the carrier fluid (3). Also, earlier models contained an assumption in the algebraic expression for the particle velocity (3) that the particles settle relative to the volume-averaged velocity of the suspension [8], and not relative to the fluid, as is the case on the two-fluid approach [2]. As a result, in contrast to the existing models the two-fluid model includes an additional term $-\nabla(wC\mathbf{V}_s)$ in the right-hand side of the pressure equation (2), which takes into account the two-speed effects.

3 Cross-flow inertial migration of particles in a fracture

Particle migration in fractures is essentially a multi-scale problem, spanning from the lift force on a single particle settling in a slot [9], through the inertial igration in a suspension flow in the horizotnal section of a fracture [10, 11] to the effects of cross-flow migration on the global transport and sedimentation in the entire fracture [12].

In thi seciton, we will consider in detail the inertial migration of particles in a dilute suspension flow through the entry region of a plane channel, which is important in application to modeling of proppant migration in the near-wellbore zone of the fracture. Within the two-fluid approach, an asymptotic one-way coupling model of the dilute suspension flow in the entry region of a channel is constructed in [10]. The carrier phase is a viscous incompressible Newtonian fluid, and the dispersed phase consists of identical non-colloidal rigid spheres. In the inter-phase momentum exchange, we take into account the drag force, the virtual mass force, the Archimedes force, and the inertial lift force with a correction factor due to the wall effect and an arbitrary particle slip velocity. The channel Reynolds number is high and the particle-to-fluid density ratio is of order unity or significantly larger unity. The solution is constructed using the matched asymptotic expansions method. The problem of finding the far-downstream cross-channel profile of particle number concentration is reduced to solving the equations of the two-phase boundary layer developing on the channel walls. The full Lagrangian approach is used to study the evolution of the cross-flow particle concentration profile.

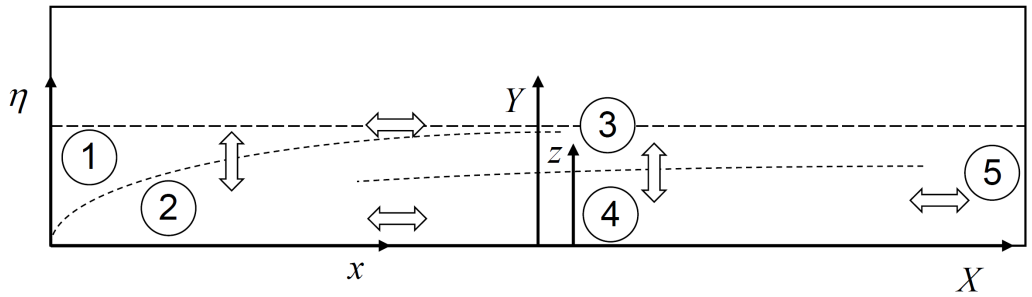

Figure 2: Asymptotic domains in the suspension flow in the horizontal section of an entry region of a fracture: *1* – the entry region, *2* – the boundary layer, *3* – the region of overlapping of the boundary layers, *4* – the lower sublayer, *5* – the far downstream region of the fully developed Poiseuille flow. Symbol ⇔ defines asymptotic matching of solutions in adjacent domains.

The system of equations of the two-phase boundary layer are as follows [10]:

$$\frac{\partial u}{\partial x}+\frac{\partial v}{\partial \eta}=0, \quad \frac{\partial \rho_s u_s}{\partial x}+\frac{\partial \rho_s v_s}{\partial \eta}=0, \qquad (4)$$
$$u\frac{\partial u}{\partial x}+v\frac{\partial u}{\partial \eta}=\frac{\partial^2 u}{\partial \eta^2}, \quad \frac{\partial p}{\partial \eta}=0,$$

$$u_s\frac{\partial u_s}{\partial x}+v_s\frac{\partial u_s}{\partial \eta}=F_{sx}=\frac{2\xi}{2\xi+1}D_0(u-u_s)+\frac{3}{2\xi+1}\left(u\frac{\partial u}{\partial x}+v\frac{\partial u}{\partial \eta}\right),$$
$$u_s\frac{\partial v_s}{\partial x}+v_s\frac{\partial v_s}{\partial \eta}=F_{s\eta},$$

$$F_{s\eta} = \frac{2\xi}{2\xi+1}\left[D_0(v-v_s) + \kappa_0 c_l\sqrt{\frac{\partial u}{\partial \eta}}(u-u_s)\right] + \frac{3}{2\xi+1}\left(u\frac{\partial v}{\partial x} + v\frac{\partial v}{\partial \eta}\right),$$

$$c_l(\chi, x, \eta) = c_l^{\infty}\left[1 - n\exp\left(-m_1(\chi)\frac{\eta}{x^{1/4}}\right)\right],$$

$$m_1 = m\frac{\sqrt{\varphi''(0)}}{(\varepsilon\lambda)^{1/4}}, \quad \chi = \frac{|u-u_s|}{(\varepsilon\lambda)^{1/4}}, \quad \xi = \rho_p^0/\rho_f^0$$

$$\kappa_0 = \frac{6.46}{12\sqrt[4]{18\pi}} Re_{s0}^{3/2}\left(\frac{\rho_s^0}{\rho}\right)^{1/4}, \quad D_0 = 1 + \frac{1}{6}Re_{s0}^{3/2}(u-u_s)^{3/2}, \quad \mathrm{Re}_{s0} = \frac{2aU\rho}{\mu}.$$

Here the latter terms in the right-hand side of the momentum conservation equations for the particulate phase correspond to the virtual mass force and the Archimedes force. Additionally, φ is the Blasius function from the well known solution of the boundary layer problem [13]. External flow is uniform, hence the longitudinal pressure gradient is zero. Boundary conditions take the form:

$$\begin{aligned} x = 0: \quad & u_s = \rho_s = 1, \quad v_s = 0; \\ \eta = 0: u = v = 0; \quad & \eta \to \infty: \quad u \to 1. \end{aligned} \tag{5}$$

The inertial migration in the entry region of a plane channel (a circular pipe) results in particle accumulation on two symmetric planes (an annulus) distanced from the walls, with a non-uniform concentration profile between the planes (inside the annulus) and particle-free layers near the walls. When the particle-to-fluid density ratio is of order unity, an additional local maximum of the particle concentration on inner planes (an inner annulus) is revealed. The inclusion of the corrected lift force makes it possible to resolve the non-integrable singularity in the concentration profile on the wall, which persisted in all previously published solutions for the dilute-suspension flow in a boundary layer [14]. The numerical results are compared with the tubular pinch effect observed in experiments, and a qualitative analogy is found.

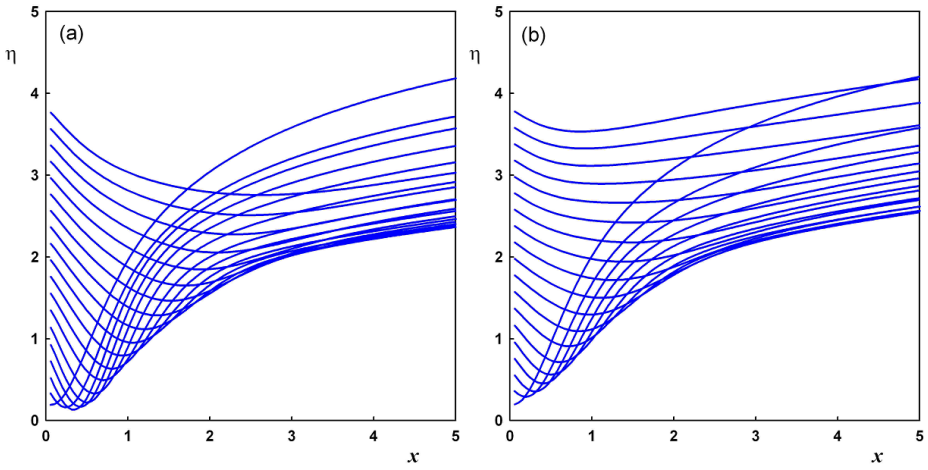

Figure 3: Trajectories of the particles in the boundary layer for the nondimensional intensity of the lift force $\kappa_0 = 20$, the particle-to-fluid density ratio $\xi = 3$ (a) and $\xi = 5$ (b).

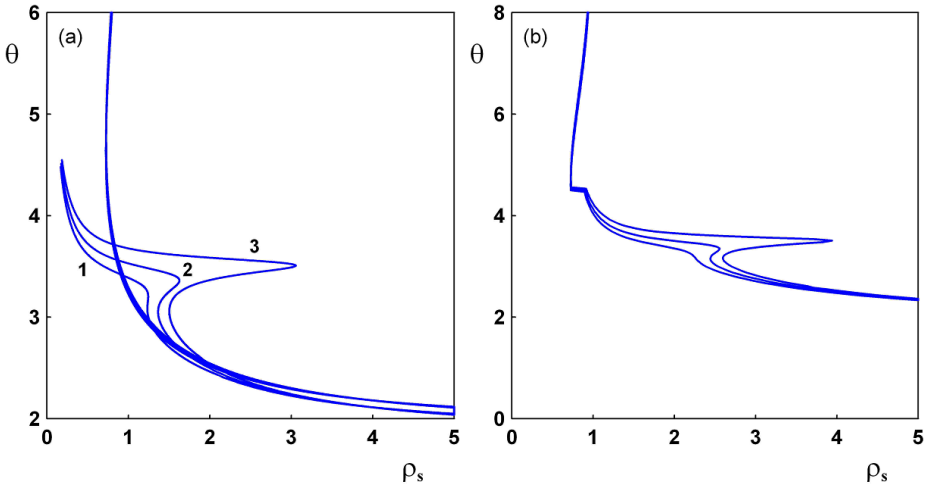

Figure 4: Far-downstream asymptotics of the cross-flow concentration profile ρ_s depending of the stream function θ in the boundary layer, $\kappa_0 = 20$ and $\xi = 5$, 4.5, Рч 4 – curves *1-3*. Profiles in each layer of the fold (a) and the total concentration profile (b).

In this case the trajectories shown in Fig. 3 are substantially different from the case of a dusty gas. The reason is that in the case of a suspension the particle-to-fluid density ratio is of order unity $\xi \sim 1$, and the terms due to the Archimedes force and the virtual mass force should be retained in the momentum conservation laws. These terms result in the formation of an additional local maximum in the cross-flow concentration profile (see Fig. 4,(a)).

4 Suspension filtration in proppant packings in a closed fracture

Suspension flow in the propped fracture is described within the three-continua approach: suspended partices (solid particles carried by the flow of a fluid within the porous space), trapped particles (solid particles, which are sedimented in pores), and carrier fluid (viscous incompressible Newtonian fluid). Suspended particles are characterised by the phase density ρ_p^{mob} and the mass-averaged velocity U_p^{mob}; the phase of trapped particles is characterized by the density ρ_p^{sed}; the carrier phase is characterised by the mass-averaged velocity U_f and density ρ_f. Particles have constant substance density ρ_p^0, and the fluid – a constant substance density ρ_f^0. Multi-continua modeling of suspension flows is applicable if the following hierarchy of scales exists: particle diamter is significantly smaller than the diameter of pore channels, while being significantly larger than the mean free path of the fluid molecules [1]. Large pore channels are the pore space excluding trapped particles and the void space between those. Small pore channels are pore space between trapped particles (Fig. 5, b).

Density of the particle phases are related to the porosity and the particle concen-

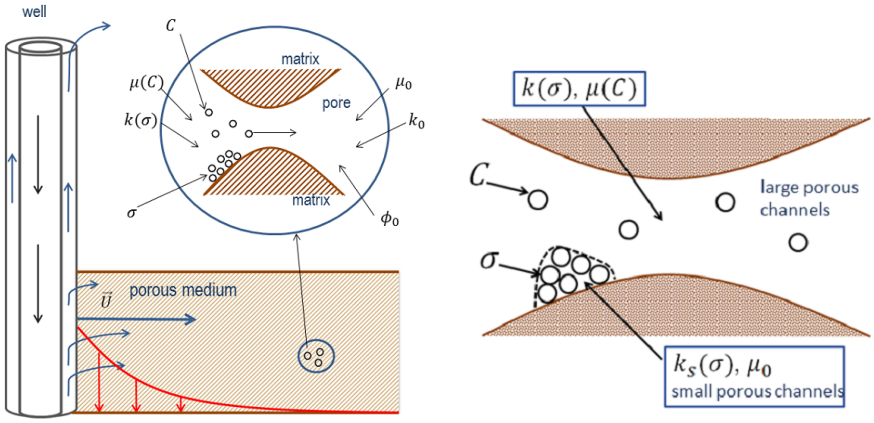

Figure 5: The sketch of suspension flow in a porous medium (a); a scheme of the porous space (b): large pore channels (1) and small pore channels (2).

tration by the following relations [15]:

$$\rho_p^{mob} = \rho_p^0 C\phi_c, \qquad \rho_p^{sed} = \sigma\rho_p^0, \qquad \rho_f = \rho_f^0(\phi_t - C\phi_c),$$

$$\phi_t = \phi_0 - \sigma, \qquad \phi_c = \phi_0 - \sigma/C_{max}, \tag{6}$$

where C is the particle volume fraction in the pore space available for the fluid to flow (in large pore channels), σ – the volume concentration of trapped particles in the entire volume of the porous medium, C_{max} is the maximum packing concentration (random close packing), ϕ_t – the porosity of the medium formed by the trapped particles and the matrix (large and small channels in total), ϕ_c – the porosity of the medium formed by the large pore channels; ϕ_0 – initial porosity of the medium.
The mass conservation equation for particles and fluid is written as [19]:

$$\frac{\partial\rho_p^{mob}}{\partial t} + \frac{1}{r^j}\frac{\partial(\rho_p^{mob}U_p^{mob}r^j)}{\partial r} = -q_s, \qquad \frac{\partial\rho_p^{sed}}{\partial t} + \frac{1}{r^j}\frac{\partial(\rho_p^{sed}U_p^{sed}r^j)}{\partial r} = q_s, \tag{7}$$

$$\frac{\partial\rho_f}{\partial t} + \frac{1}{r^j}\frac{\partial(\rho_f U_f r^j)}{\partial r} = 0.$$

Here $j = 0$ in a plane flow and $j = 1$ in a radial flow, q_s is the rate of trapping and mobilization of particles in the matrix, determined by the formulas [16]:

$$q_s = \rho_p^{mob}U_p^{mob}\lambda - \rho_p^0\alpha\sigma\delta(U_s - U_{crit}), \tag{8}$$

$$\delta(U_s - U_{crit}) = \begin{cases} U_s - U_{crit}, & U_s > U_{crit} \\ 0, & U_s < U_{crit} \end{cases}.$$

Here λ is the colmatation coefficient (intensity of particle trapping) [20], α – the coefficient of mobilization of trapped particle, U_s is the filtration velocity in large and small pore channels, U_{crit} is the critical suspension velocity, above which trapped particles are mobilized.

In large pore channels with the permeability $k(\sigma)$, the suspension is flowing with the viscosity $\mu(C)$. In small pore channels with the permeability $k_s(\sigma)$, only the clean fluid is flowing with the dynamic viscosity μ_0. The momentum conservation equations (Darcy laws) for the carrier phase, suspended particles and the suspension as a whole are obtained by volume-averaging in large and small pore channels:

$$U = -\frac{k(\sigma)}{\mu(C)}\frac{\partial p}{\partial r}, \qquad U_s = -\left[\frac{k(\sigma)}{\mu(C)} + \frac{k_s(\sigma)}{\mu_0}\right]\frac{\partial p}{\partial r}, \tag{9}$$

$$U_f^{filtr} = -\left[(1-C)\frac{k(\sigma)}{\mu(C)} + \frac{k_s(\sigma)}{\mu_0}\right]\frac{\partial p}{\partial r}, \qquad U_p = -C\frac{k(\sigma)}{\mu(C)}\frac{\partial p}{\partial r},$$

$$U_f^{filtr} = U_f(\phi_t - C\phi_c).$$

Here U is the suspension filtration velocity in large and small pores, U_f^{filtr} is the fluid filtration velocity in large and small pore channels, $U_p = U_p^{mob} C\phi_c$ is the volume-averaged velocity of suspended particles in large pore channels, p – pressure.
The work [3] suggests the following relation between the permeability in large pore channels and the volume fraction of trapped particles:

$$k(\sigma) = k_0\left(1 - \frac{\sigma}{\phi_0 C_{max}}\right)^3. \tag{10}$$

Permeability in small pore channels:

$$k_s = k_{s0}\left(\frac{\sigma}{\phi_0 C_{max}}\right)^3, \qquad k_{s0} = \frac{(1-C_{max})^3 d^2}{180 C_{max}^3}. \tag{11}$$

Here k_{s0} is the permeability of small pore channels during full packing of porous space ($\sigma = \phi_0 C_{max}$), determined from the Kozeny-Carman formula [21]; d is the diameter of particles in suspension.
Using the definitions introduced above, the conservation equations can be reformulated as:

$$\frac{\partial(C\phi_c)}{\partial t} + \frac{1}{r^j}\frac{\partial(CUr^j)}{\partial r} = -UC\lambda + \alpha\sigma\delta(U_s - U_{crit}), \tag{12}$$

$$\frac{\partial \sigma}{\partial t} = UC\lambda - \alpha\sigma\delta(U_s - U_{crit}),$$

$$\frac{\partial(U_s r^j)}{\partial r} = 0.$$

Classical deep-bed filtration models of suspension flow do not take into account the fact that the particles trapped in pores form a secondary porous medium (a random close packing of sedimented particles) with the permeability smaller than the permeability of the matrix. Filtration through the close packing of trapped particles is not considered in the classical models.

Below for comparison we present the classical model of deep-bed filtration in large pore channels without considering the flow in small pore channels in the packed bed of trapped particles ($\phi_c = \phi_t = \phi_0 - \sigma, U = U_s, k_s = 0$) [3, 5, 15, 24, 18]:

$$\frac{\partial(C\phi_c)}{\partial t} + \frac{1}{r^j}\frac{\partial(CUr^j)}{\partial r} = -CU\lambda(\sigma) + \alpha\sigma\delta(U - U_{crit}),$$
$$\frac{\partial\sigma}{\partial t} = CU\lambda(\sigma) - \alpha\sigma\delta(U - U_{crit}),$$
$$\frac{\partial(Ur^j)}{\partial r} = 0, \qquad U = -\frac{k(\sigma)}{\mu(C)}\frac{\partial p}{\partial r}. \tag{13}$$

Experiments on colmatation of core sample [23] have shown that the model (13) can be improved by introducing the following expression:$\lambda = \lambda_0(1+\beta\sigma)$. Here, λ_0 is the original colmatation coefficient. Thus, the classical model (13) contains two tuning parameters λ_0 Рч β.

Two versions of boundary conditions are considered: - (i) pressure is specified at the entry and at the outlet of the core sample (a): $r = r_0 : p = p_0, C = C_0$; $r = L : p = 0$. - (ii) the filtration velocity is specified at the inlet, and pressure – at the outlet (b): $r = r_0 : U_s = U_0, C = C_0$; $r = L : p = 0$.

Initial conditions: $t = t_0 : \phi = \phi_0, \sigma = 0$.

Closure relations for permeability of the random close packing of proppant in a hydraulic fracture can be found from direct numerical simulation supported by proper conductivity experiments (see, for example, LBM simulations in mixed packing of proppant particles of various shape in [25]).

5 Gas-liquid flows in a well during cleanup

In this section we will discuss the first-principles derivation of simplified drift-flux equations for gas-liquid flows in a well [26]. We consider a transient isothermal flow of a gas-liquid mixture in a long circular pipe with a variable inclination angle to the horizon. The flow is assumed to be axisymmetric and non-swirling. The liquid is a continuous carrier phase. The gas is a dispersed phase present in the form of monodisperse spherical bubbles suspended in the carrier fluid. The gas is compressible, and the liquid is incompressible. The cross-flow migration of the bubbles and their merging are not considered; however, we take into account the resulting nonuniform cross-flow profile of the gas volume fraction, which is formed as a result of the migration of the bubbles. The pressure difference in the bubbles and in the surrounding liquid due to surface tension is neglected. The bubble size is assumed to be much smaller than the spatial scales of variation of the fluid velocity, and the Reynolds numbers of the flow around individual bubbles are small.

The two-phase flow is considered within the approach of interpenetrating and interacting continua [1]. The problem is described by conservation laws in differential form, written for gas and liquid phases. The mass transfer between the phases is absent.

The balance laws of mass and momentum in the differential form for gas and liquid

take the form [1]:

$$\frac{\partial}{\partial t}(\alpha_i \rho_i) \; + \; \nabla(\alpha_i \rho_i \mathbf{v}_i) = 0 \tag{14}$$

$$\alpha_i \rho_i \frac{d_i \mathbf{v}_i}{dt} = -\nabla p_i \; + \; \nabla \cdot \boldsymbol{\phi}_i \; + \; \alpha_i \rho_i \mathbf{g} \; + \; n_b \mathbf{F}_{ij} \tag{15}$$

$$\frac{d_i}{dt} = \frac{\partial}{\partial t} \; + \; (\mathbf{v}_i \cdot \nabla).$$

Here, the indexes $i, j = g, l$ $(i \neq j)$ denote gas and liquid, respectively, α_i, ρ_i, and $\mathbf{v}_i$ are the volume fractions, densities and velocities of the phases, p_i and $\boldsymbol{\phi}_i$ are the pressures and viscous stress tensors in each phase, and $\mathbf{g}$ is the gravity force acceleration. The momentum exchange between the phases is described by the term $\pm n_b \mathbf{F}_{ij}$, where $\mathbf{F}_{gl} = \mathbf{F}$ is the force exerted on a single bubble by the fluid, $\mathbf{F}_{lg} = -\mathbf{F}_{lg}$, and n_b is the number concentration of the bubbles.

For simplicity, the following calculations are performed for a vertical pipe, although the results may be generalized to the case of an inclined pipe, excluding flows in near-horizontal pipes.

It is assumed that the chaotic motion of the bubbles can be neglected, and the deviation of the bubble velocity from the mass-averaged velocity of the dispersed phase $\mathbf{v}_g$ is small, hence the stress tensor in the dispersed phase can be neglected [2]. The presence of the dispersed phase affects the stress tensor of the carrier phase. On the other hand, the bubbles of a compressible gas travel with a velocity different from that of the fluid, and the bubble volume fraction varies. Accordingly, the condition $\nabla \mathbf{v}_l = 0$ is no longer true. In this sense, the averaged liquid phase is compressible, in contrast to the liquid as a material. Therefore, the stress tensor of the carrier phase is written as for a viscous compressible fluid, with the coefficients of shear viscosity μ and bulk viscosity ζ dependent on the gas volume fraction:

$$\boldsymbol{\phi}_l = 2\mu(\alpha_g)\left(\mathbf{e}_l \; - \; \frac{1}{3}\nabla \mathbf{v}_l \mathbf{I}\right) \; + \; \zeta(\alpha_g)\nabla \mathbf{v}_l \mathbf{I}.$$

Here, $\mathbf{e}_l$ is the strain rate tensor, and I is the unit tensor. To determine the dependences $\mu(\alpha_g)$ and $\zeta(\alpha_g)$ is a separate problem, which is usually solved for neutrally-buoyant particles, neglecting the phase slip. In what follows, we assume that $\mu(0) = \mu_0$, where μ_0 is the viscosity of the pure fluid, and $\zeta(\alpha_g)\nabla \mathbf{v}_l \to 0$ as $\alpha_g \to 0$.

The bubble radius is bounded by a limiting value R_c above which the bubble loses the spherical shape, becomes unstable, and is fragmented into smaller bubbles:

$$R \leq R_c \simeq \frac{1}{3}\left(\frac{\sigma}{\rho_l g}\right)^{\frac{1}{2}} \simeq 10^{-3}\text{m}.$$

Here, σ is the gas-liquid surface tension. Under the above assumptions, the total force exerted on a bubble by the fluid is a superposition of the Stokes $\mathbf{F}_s$, the Archimedes $\mathbf{F}_A$, the added mass $\mathbf{F}_{am}$, and the Basset-Boussinesq $\mathbf{F}_{BB}$ forces. Accordingly, the forces on a bubble can be written in the form:

$$\mathbf{F} = \mathbf{F}_{St} \; + \; \mathbf{F}_A \; + \; \mathbf{F}_{am} \; + \; \mathbf{F}_{BB}$$

$$\mathbf{F}_{St} = 6\pi\mu R(\mathbf{v}_l - \mathbf{v}_g), \quad \mathbf{F}_A = \frac{4}{3}\pi R^3\rho_l\left(\frac{d_l\mathbf{v}_l}{dt} - \mathbf{g}\right), \quad \mathbf{F}_{am} = \frac{2}{3}\pi R^3\rho_l\frac{d_g}{dt}(\mathbf{v}_l - \mathbf{v}_g)$$

For a transient flow in a well, the equations of the drift-flux model, known in the literature and implemented in the commercial reservoir simulator ECLIPSE (Schlumberger), take the form [27, 28]:

$$\frac{\partial}{\partial t}(A\alpha_i\rho_i) + \frac{\partial}{\partial z}(A\alpha_i\rho_i v_i) = 0 \tag{16}$$

$$\rho_m\left(\frac{\partial v_m}{\partial t} + v_m\frac{\partial v_m}{\partial z}\right) = -\frac{\partial p}{\partial z} + \rho_m g\cos\theta + \frac{2f\rho_m v_m|v_m|}{d} \tag{17}$$

$$v_g = C_0 v_m + v_d. \tag{18}$$

Here, A is the pipe cross-section, $v_m = \alpha_g v_g + \alpha_l v_l$ is the volume-averaged velocity of the mixture, $\rho_m = \alpha_g\rho_g + \alpha_l\rho_l$ is the mixture density, $f = f(\alpha_g, v_m, p)$ is the friction coefficient, d is the pipe diameter, and θ is the angle between the pipe axis and the vertical.

In the applications, a quasi–steady-state variant of the drift-flux model is widely used, in which the time-derivative in the momentum equation for the mixture is neglected and the total pressure difference is equal to the sum of the terms responsible for the gravity force, friction, and acceleration [27]. In the literature, this model is referred to as the no-pressure wave model, since it does not take into account the disturbance propagation with the transport velocity. In contrast to this quasi–steady-state formulation, we retain the time derivative of velocity in the momentum equation to take into account highly transient effects.

In the literature, formula (18) [1] (where $C_0 = C_0(\alpha_g, v_m, p)$ is the profile parameter which takes into account a non-uniform cross-flow profile of the bubble volume fraction and the carrier-phase velocity, and $v_d = v_d(\alpha_g, v_m, p)$ is the drift velocity) is called the drift-flux model relation.

There is also another known formulation of the drift-flux model [29], with the mixture momentum equation written as

$$\frac{\partial}{\partial t}(\alpha_g\rho_g v_g + \alpha_l\rho_l v_l) + \frac{\partial}{\partial z}(\alpha_g\rho_g v_g^2 + \alpha_l\rho_l v_l^2 + p) = Q_l + Q_g, \tag{19}$$

where Q_i are the source terms for each phase, and the drift-flux relation written as

$$v_g - v_l = \Phi(\alpha_g, v_g, p) \tag{20}$$

The asymptotic equations are derived in the long-channel approximation $\varepsilon \ll 1$, similar to the boundary-layer approximation, the narrow-channel approximation for fracturing flows [2], and the lubrication approximation for thin-film flows [30].

To come up with an algebraic relation between the phase velocities, additionally it is assumed that

$$\varepsilon\mathrm{St}\eta \ll 1, \quad \eta \gg 1, \quad \frac{\mathrm{St}}{\mathrm{Fr}^2}\eta \sim 1, \quad \varepsilon\mathrm{Re} \sim 1, \ \varepsilon\xi_0 \ll 1.$$

Thus, the drift-flux model in the form (16)-(18) can be derived from conservation laws only in the following three cases: (i) small volume fraction of the dispersed phase $\alpha \ll 1$; (ii) no phase velocity slip $|C_0 - 1| \ll 1$, $\eta \mathrm{St}/\mathrm{Fr}^2 \ll 1$; and (iii) inertialess flows $\varepsilon \mathrm{Re} \ll 1$.
Our analysis demonstrates that the drift-flux model [27, 28] in the form (16)-(18) for the present flow configuration strictly follows from the conservation laws in the limited number of cases (i)-(iii) and represents essentially the effective-fluid model. The closure relations published in open literature are obtained from a calibration against a large body of experimental data [27, 28] for the governing parameters satisfying at least one of conditions (i)-(iii). At the same time, our analysis indicates that the drift-flux model [29] in the form (16), (19), and (20) is more general because it follows from the balance laws without any additional assumptions, besides the requirement of noninertial slip $\varepsilon \mathrm{St} \ll 1$.

6 Conclusions

We review a family of closely-related multi-scale models derived by the author from conservation laws within the multi-fluid approach using perturbation methods to describe all stages of the technology of hydraulic fracturing. The models cover suspension injection into the well to create primary fractures, suspension transport and sedimentation in a fracture, cross-flow inertial migration of particles in a horizontal section of a hydraulic fracture, filtration of suspensions of non-colloidal particles in a random close packing of proppant particles in the closed fracture, and gas-liquid flows in a well during cleanup and startup. In particular, our review covers:
1. A novel two-fluid model of suspension transport in a hydraulic fracture. It is shown that the model is different from the existing effective-fluid model of suspension flow by additional terms due to two-speed effects. These terms are important at high buoyancy numbers Bu, which corresponds to the case of high-rate slick-water fracturing. In the case of conventional fracturing with high-viscosity cross-linked gels, the models match. This model is then generalized to the case of a Bingham fluid flow and validated against four different sets of experiments on slumping, Saffman-Taylor fingering in Newtonian fluids, fingering and channeling in yield-stress fluids, and suspension transport and sedimentation in a slot with formation of a packed bed of particles at the bottom.
2. A multi-scale model of particle migration in a dilute-suspension flow through the fracture is developed, including the expression for the lift force on a particle settling in a horizontal flow through a vertical slot, the model of particle migration in the entry region of a plane channel with account for the Saffman lift force on a particle with the correction due to the wall effect, the model of migration of settling particles in a fully developed Poiseuille flow in a channel. Using the full Lagrangian approach, the particle concentration profile with an integrable singularity is obtained as a solution to the problem of the two-phase boundary layer. This achievement marks the first time that a self-consistent solution is obtained for the two-phase boundary layer problem within the dilute-suspension approximation, as all earlier solutions contained a non-integrable singularity thus making the model of dilute suspension inapplicable. New 2D width-averaged equations of suspension transport in a fracture

are derived with account for the non-uniform cross-flow particle concentraiton profile formed as a result of the migration.
3. A three-continua model is constructed for the suspension flow in a porous medium with account for the effects of particle trapping and mobilization. The model takes into account the effect of trapped particles forming a secondary porous medium of random closed packing with smaller permeability. Fluid fluxe through packed trapped particles is taken into account. In order to close the model, for the first time in a wide range of porosity we derived a permeability-porosity correlation for the random close packing of non-spherical particles based on the 3D simulation of viscous flow using the lattice-Boltzmann method, validated against lab conductivity tests.
4. The derivation of asymptotic equations of the drift-flux model for a dilute gas-liquid disperse two-phase flow in a circular pipe is presented in the long-channel approximation. This asymptotic model is obtained as a limit of the full equations based on the balance laws, written for each phase in the multi-fluid approximation. The key assumptions are determined, which make it possible to derive the drift-flux model from the balance laws. This model contains an algebraic relation for the phase velocities and a single equation for the mixture momentum, written for the volume-averaged velocity of the mixture. To derive the drift-flux relation for the phase velocities, when one phase is continuous and the second dispersed, it is required to assume only that the characteristic length scale of the problem is significantly greater than the velocity relaxation length. To derive the single equation for mixture momentum, it is necessary to assume additionally that one of the following conditions is satisfied: (i) the dispersed-phase volume fraction is small, (ii) the phase velocity slip can be neglected, or (iii) the flow is inertialess, i.e. the mixture acceleration can be neglected. At the same time it is shown that the drift-flux model, in which a single mixture momentum conservation equation is obtained as the sum of two momentum conservation equations for the phases, follows from the conservation laws under one assumption that the characteristic length scale of the problem is significantly larger than the phase velocity relaxation length; hence, this model is more general.

Acknowledgements

Startup funds of Skolkovo Institute of Science and Technology are gratefully acknowledged.

References

[1] Nigmatulin, R.I., 1990. Dynamics of multiphase media (Vol. 1,2). CRC Press.

[2] Boronin, S.A. and Osiptsov, A.A., 2010. Two-continua model of suspension flow in a hydraulic fracture. Doklady Physics . 55(4), 199вЃY202.

[3] Boronin, S. A., Osiptsov, A. A., Desroches, J. 2015 Displacement of yield-stress fluids in a fracture, Intl. J. Multiphase Flow **76**, 47–63.

[4] Boronin, S.A., Osiptsov, A.A. and Tolmacheva, K.I., 2015. Multi-fluid model of suspension filtration in a porous medium. Fluid Dynamics, 50(6), pp.759-768.

[5] Krasnopolsky, B., Starostin, A. and Osiptsov, A.A., 2016. Unified graph-based multi-fluid model for gasвГYliquid pipeline flows. Computers & Mathematics with Applications, 72(5), pp.1244-1262.

[6] Osiptsov, A.A. Fluid mechanics of hydraulic fracturing: a review // *Journal of Petroleum Science & Engineering*, 2017. (*under review*).

[7] Adachi, J., Siebrits, E., Peirce, A., & J. Desroches, 2007 Computer simulation of hydraulic fractures. Int. J. of Rock Mech. and Mining Sci. **44**(1), 739–757.

[8] Pearson, J. R. A. 1994 On suspension transport in a fracture: framework for a global model. Non-Newtonian Fluid Mech. **54**, 503–513.

[9] Asmolov, E.S. and Osiptsov, A.A., 2009. The inertial lift on a spherical particle settling in a horizontal viscous flow through a vertical slot. Physics of Fluids, 21(6), p.063301.

[10] Osiptsov, A.A., Asmolov, E.S. 2008 Asymptotic Model of the Inertial Migration of Particles in a Dilute Suspension Flow Through the Entry Region of a Channel. *Phys. Fluids* **20** (1вГY2), 123301.

[11] Asmolov, E.S., Lebedeva, N.A. and Osiptsov, A.A., 2009. Inertial migration of sedimenting particles in a suspension flow through a Hele-Shaw cell. Fluid Dynamics, 44(3), pp.405-418.

[12] Boronin, S.A. and Osiptsov, A.A., 2014. Effects of particle migration on suspension flow in a hydraulic fracture. Fluid Dynamics, 49(2), pp.208-221.

[13] Schlichting, H., 1960. Boundary-layer theory. New York: McGraw-hill. Vancouver.

[14] Foster M.R., Duck P.W., Hewitt R.E. Boundary layers in a dilute particle suspension // Proc. R. Soc. A. 2006. V. 462. P. 136 вГY 168.

[15] Gruesbeck C., Collins R.E. Entrainment and deposition of fine particles in porous media // SPE Journal. 1982. N 8430. P. 847-856.

[16] Bailey L., Boek E.S., Jaques S.D.M., Boassen T., Selle O.M., Argillier J.-F., Longeron D.G. Particulate Invasion From Drilling Fluids // SPE Journal. 2000. V. 5(4). P. 412-419.

[17] Boek E.S., Hall C., Tardy P. M. J. Deep bed filtration modelling of formation damage due to particulate invasion from drilling fluids // Transport in Porous Media. 2012. V. 91(2). P. 479-508.

[18] Guedes R.G., Al-Abduwani F., Bedrikovetsky P., Currie P.K. Deep-Bed Filtration Under Multiple Particle-Capture Mechanisms // SPE Journal. 2009. V. 14(3). P. 477-487.

[19] Sedov, L.I., 1972. A Course in Continuum Mechanics: Fluids, gases and the generation of thrust. Wolters-Noordhoff.

[20] Mikhailov N.N. Variation of physical properties of rocks in the near wellbore zone [in Russian]. Moscow. Nedra, 1987.

[21] Van Der Hoef M. A., Beetstra R., Kuipers J. A. M. Lattice-Boltzmann simulations of low-Reynolds-number flow past mono- and bidisperse arrays of spheres: results for the permeability and drag force // Journal of Fluid Mechanics. 2005. V. 528. P. 233- 254.

[22] Herzig J.P., Leclerc D.M., Le Goff P. Flow of Suspensions through Porous Media // Industrial and engineering chemistry. 1970. V. 62(5). P. 9-34.

[23] Heertjes P. M., Lerk C.F. The functioning of deep bed filters // Trans. Inst. Chem. Eng. 1967. V. 45. P. 124-145.

[24] Civan F. Reservoir Formation Damage. Gulf Professional Publishing. Elsevier Inc. 2007. 1135 CF.

[25] Osiptsov, A.A. Hydraulic fracture conductivity: effects of non-spherical proppant from lattice-Boltzmann simulations and lab tests // *Advances in Water Resources*, 2017. (*accepted*).

[26] Osiptsov, A.A., Sinвґєkov, K.F. and Spesivtsev, P.E., 2014. Justification of the drift-flux model for two-phase flow in a circular pipe. Fluid Dynamics, 49(5), pp.614-626.

[27] A.R. Hasan and C.S. Kabir, *Fluid Flow and Heat Transfer in Wellbores* (Society of Petroleum Engineers, Richardson, Texas, 2002).

[28] H. Shi, J.A. Holmes, L.J. Durlofsky, et al., “Drift-Flux Modeling of Two-Phase Flow in Wellbores," SPE J. **10**, 24–33 (2005).

[29] S. Evje and T. Flatten, “On the Wave Structure of Two-Phase Models," SIAM J. Appl. Math. **67**, 487–511 (2007).

[30] A.A. Osiptsov, Steady Film Flow of a Highly Viscous Heavy Fluid with Mass Supply, Fluid Dynamics **38** (6), 846-853 (2003).

[31] Zhibaedov, V.D., Lebedeva, N.A., Osiptsov, A.A. and Sinвґєkov, K.F., 2016. On the hyperbolicity of one-dimensional models for transient two-phase flow in a pipeline. Fluid Dynamics, 51(1), pp.56-69.

Andrei A. Osiptsov, Skolkovo Institute of Science and Technology, Nobel Street 3, 143026 Moscow, Russia